Title	The effect of Ga-doped nanocrystalline ZnO electrode on deep-ultraviolet enhanced GaN photodetector
Author(s)	Wang, RX; Yang, LC; Zhang, YM; Xu, S; Fu, K; Zhang, BS; Wang, J; Xu, K; Yang, H
Citation	Applied Physics Letters, 2013, v. 102, p. 212104:1-4
Issued Date	2013
URL	http://hdl.handle.net/10722/186162
Rights	Applied Physics Letters. Copyright © American Physical Society.

The effect of Ga-doped nanocrystalline ZnO electrode on deep-ultraviolet enhanced GaN photodetector

R. X. Wang,[1,a)] L. C. Yang,[1] Y. M. Zhang,[1] S. J. Xu,[1,2] K. Fu,[1] B. S. Zhang,[1] J. F. Wang,[1] K. Xu,[1] and H. Yang[1]

[1]*Key Laboratory of Nanodevices and Applications, Suzhou Institute of Nano-tech and Nano-bionics, Chinese Academy of Sciences, Suzhou 215123, China*

[2]*Department of Physics and HKU-CAS Joint Laboratory on New Materials, The University of Hong Kong, Pokfulam Road, Hong Kong, China*

(Received 19 January 2013; accepted 17 May 2013; published online 31 May 2013)

Two types of GaN-based ultraviolet (UV) photodetectors were fabricated by using NiAu and Ga-doped ZnO (GZO) as electrode materials, respectively. Dark current-voltage and photoresponse characteristics of the devices were investigated. It is found that in addition to the ~365 nm cut-off response of GaN, an enhanced responsivity at around 250 nm is achieved for the GZO/GaN photodetectors. Photo absorption measurements provide proof that the efficient deep UV absorption occurs in the solar blind spectral zone. Transmission electron microscopy observations reveal the existence of nanostructures in the GZO thin film. Such nanostructures could be responsible for the deep UV photoresponse. © *2013 AIP Publishing LLC*. [http://dx.doi.org/10.1063/1.4808381]

In the past decade, ultraviolet (UV) photodetectors (PDs), especially solar blind PDs, have attracted a great deal of interest because of their wide applications in military and civil detections and monitoring.[1–4] In order to fabricate solar blind PDs, active materials with optical responding wavelength less than 280 nm shall be employed. GaN based materials are suitable for preparing the UV and solar blind UV PDs. In the past, various GaN-based structures, such as Schottky contacts, metal-semiconductor-metal (MSM), and p-i-n structures have been investigated for preparing UV PDs.[5–8] Metallic materials are common in the fabrication of electrodes for these device structures. However, as opaque metal electrodes block more light; transparent conductive electrodes could be used to obtain higher efficiency of optical to electrical conversion in PDs. Some transparent oxides such as tin-doped indium oxide (ITO) and Ga-doped zinc oxide (GZO) have been demonstrated to have exceptional electrical conductivity and optical transparency.[9–11] As oppose to ITO, GZO is more advantageous due to its lower cost and stability.[12,13] In this letter, we report a comparative study on the characteristics of two types of GaN-based UV PDs prepared using two different electrode materials: NiAu and GZO. The GZO/GaN PDs show dramatically enhanced deep-UV photoresponse.

Semi-insulating GaN epitaxial wafers used in this study were grown with hydride vapor phase epitaxy (HVPE). Prior to making electrode contacts, the GaN wafer was cleaned by immersing the sample sequentially in acetone, ethanol, and de-ionized water in ultrasonic oscillators. In order to remove native oxide and contamination, the GaN wafer was dipped into different acid solution and then rinsed in de-ionized water and finally dried with N_2. After these treatments, interleaved fork-shape MSM type PDs were prepared with two different electrode materials, NiAu thin films were deposited by e-beam evaporation and GZO thin films were sputtered with radio-frequency magnetron sputtering, respectively. Standard lift-off processes were then used to make the interleaved fork-shape electrode structures. The two kinds of PDs have the same electrode pattern structure with layout image as shown in Fig. 1. The central pattern was $500 \times 500\ \mu m^2$ with 1:1 electrode finger width/spacing. The thickness of the GZO thin film was ~100 nm. For the convenience of discussion, NiAu/GaN and GZO/GaN PDs are denoted as S1 and S2, respectively.

Room-temperature dark current-voltage (I-V) characteristics of the prepared PDs were measured using Keithley 4200 parameter analyzer. The spectral responsivity of the PDs was measured using a Xe arc lamp plus a calibrated monochromator as a light source. Output power of the monochromatic light was calibrated with a commercial Si PD. The spectral responsivity measurements were carried out at different applied bias for the PDs. The cross sectional microstructures of S2 device were observed by Tecnai G^2 F20

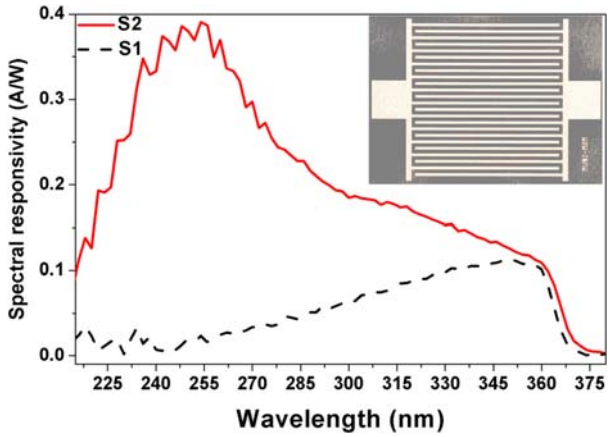

FIG. 1. Measured spectral responsivity curves of NiAu/GaN (dashed line) and GZO/GaN (solid line) photodetectors. The inset shows the top-view photo of the device electrode pattern.

[a)]Author to whom correspondence should be addressed. E-mail: rxwang2008@sinano.ac.cn

S-Twin high resolution transmission electron microscope (TEM). The crystallization structures of the films on sapphire substrate were examined with a Bruker D8 advance x-ray diffractometer (XRD) at room temperature.

Figure 1 shows the measured spectral responses of S1 and S2 at room temperature. The inset shows a top-view image of the device electrode pattern. As mentioned earlier, the two types of devices are identical in electrode pattern and size. From Fig. 1, it can be seen that both S1 and S2 show a similar sharp cut-off response at around 365 nm wavelength in correspondence to the band edge of GaN, which is consistent with the results reported by other groups.[5,7,8] However, large difference exists between the spectral response characteristics of the two samples. S1 exhibits a responsive peak at around 350 nm and low response in the deep UV region, while S2 shows a much broader spectral response, especially a strong peak at around 250 nm. This indicates the remarkable enhancement in responsivity at around 250 nm in S2.

In order to explore and investigate the origin of such responsivity enhancement in S2, room-temperature *I-V* characteristics of the samples were measured under controlled dark and illuminated conditions. The results are shown in Fig. 2. The solid lines are the dark I-V curves of the devices without light illumination, while the symbol lines represent the *I-V* characteristics of the devices under illumination at 250 nm deep UV light. The NiAu/GaN and GZO/GaN PDs exhibit very different characteristics. For dark current, S1 device was advantageous due to good NiAu/GaN Schottky contacts, whereas for photocurrent, S2 device performed much better.

For MSM structured Schottky-type PDs, the dark current is mainly determined by the reverse leakage current of the Schottky contact. Under a 10.0 V bias voltage, the typical dark currents of S1 and S2 were around 2.0 nA and 332.0 nA. It is evident that the dark current of S1 is much smaller than S2 although both devices have the same electrode patterns and size. As mentioned earlier, the deposition of NiAu contacts in S1 was done by e-beam evaporation while GZO contacts in S2 were prepared by radio-frequency magnetron sputtering. It is known that sputtering could induce more damage on the sample surface/interface than thermal evaporation, thus the larger dark current observed in S2 can be attributed to the interface damage by Ar^+ plasma during the GZO deposition. In addition to this mechanism, difference in the barrier height between the GZO/GaN and NiAu/GaN contacts could be another important factor causing the large difference in dark current between the two types of devices. Based on the well-known thermal emission model,[10,14] the dark current of a metal-semiconductor Schottky contact shows a distinct exponential dependence on the contact barrier height, i.e., $I_d \propto e^{-q\phi/kT}$, where $q\phi$ is the barrier height, k is the Boltzmann constant, and T is the temperature. In the present study, the barrier height of the GZO/GaN contact could be smaller than that of the NiAu/GaN contact.[10,15] The lower barrier height of the GZO/GaN contact could also result in the larger dark current for device S2.

The photocurrents of the two devices under the illumination of 250 nm deep UV light are also depicted in Fig. 2 for comparison. The photocurrent of S2 is much greater than that of S1 in the solar blind spectral zone. Strongly enhanced deep UV photoresponse of GZO/GaN PDs suggests that the GZO electrodes could also be used as an efficient deep UV sensitive layer. To test the idea and mechanism behind the phenomenon, high-resolution TEM observation was carried out for S2. Figure 3 shows a typical cross-sectional TEM image of the GZO layer on GaN. It can be seen that the GZO contact layer contains amorphous matrix and a large quantities of nanocrystals with size of several nanometers. These nanocrystals play a key role in the observed deep UV photoresponse of S2. During the sputtering process, Ga, Zn, and O kicked out by high energy ions arrive on the substrate surface and collide with the surface atoms. Such surface bombardment transfers certain kinetic energy, influencing the surface of GaN substrate and the formation of GZO film. The incorporation of Ga during the sputtering not only works as dopants but also plays an important role in the observed enhancement of responsivity in the solar blind spectral zone for S2. It has been reported that Ga can react with oxygen to form gallium oxides with natural band gap of about 4.4–5.0 eV[16,17] and help to form

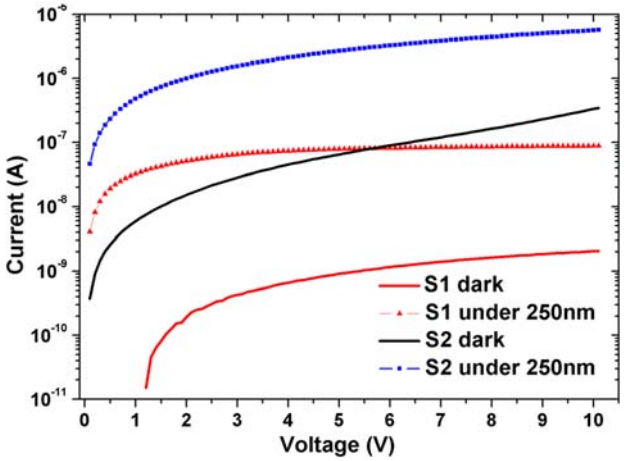

FIG. 2. Measured I-V curves of S1 and S2 photodetectors under the dark condition and light illumination of monochromatic light at 250 nm.

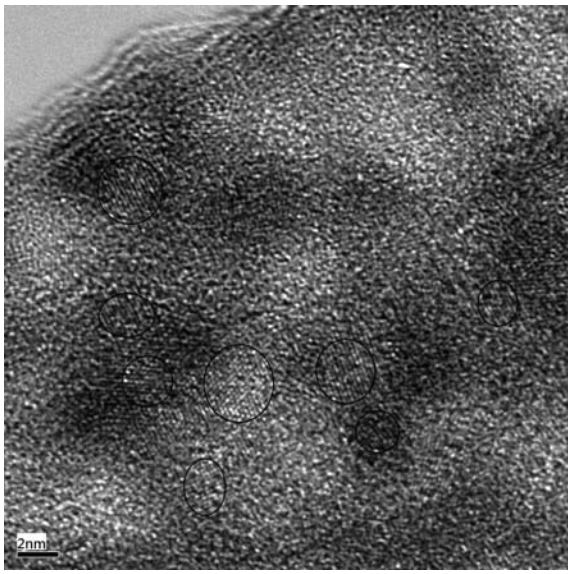

FIG. 3. Cross sectional TEM image of GZO thin film on GaN. Nanocrystals (circled regions) can be clearly resolved in the GZO thin film.

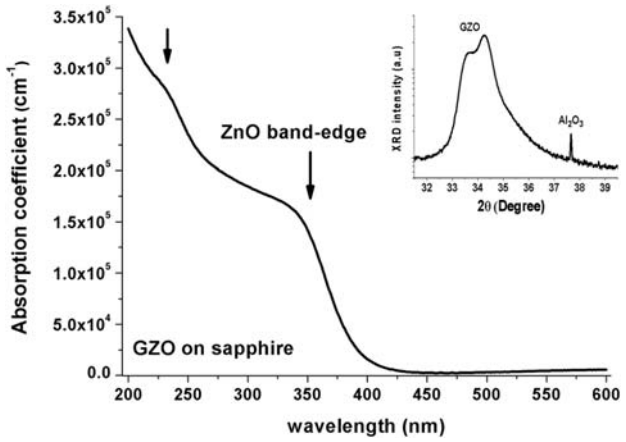

FIG. 4. The absorption coefficient of the GZO film sputtered on sapphire vs. the wavelength. The inset shows the XRD patterns of the film.

intermediate phases between wurtzite ZnO and spinel $ZnGa_2O_4$ with bandgap around 4.4–4.7 eV.[18,19] In addition, the nanocrystals embedded in the GZO thin film may have noticeable quantum confinement and size effects which results in an obvious blue shift of the band gap.[20]

In order to further investigate the microstructures of sputtered GZO thin film and the deep UV photoresponse mechanism, we measured the absorption coefficient and the XRD patterns of the GZO film deposited on sapphire under the same sputtering conditions. Figure 4 shows the measured room-temperature absorption coefficients of the GZO thin film on sapphire as a function of wavelength. A new absorption band is observed at around 250 nm in addition to the band-edge absorption of ZnO at around 360 nm, giving direct evidence of the efficient deep UV photoresponse of the GZO thin film. The inset figure depicts the XRD patterns of the film, having two distinct peaks, which gives unambiguous evidence of the mixture phase of the film.

Finally, we turn to discuss the photocurrent in S2. It is known that the optical responsivity R_{ph} is dependent on the gain G_L of photodetectors as follows:[14,21]

$$R_{ph} = \frac{qG_L(L_n + L_p)}{P_{opt}}, \tag{1}$$

$$G_L \propto \alpha(\lambda)\exp[-\alpha(\lambda)d], \tag{2}$$

$$L_{n(p)} = \sqrt{D_{n(p)}\tau_{n(p)}}, \tag{3}$$

where q, $\tau_{n(p)}$, $D_{n(p)}$, α, λ, and d represent the electron charge, the lifetimes of carriers (electron or hole), the diffusion coefficients of carriers, the absorption coefficient, the incident light wavelength, and the depth of incident light wavelength penetration, respectively. Under light illumination, photo absorption excited excess carriers (i.e., electrons in conduction band and holes in valence band) in the active layer will move toward the collection area under the influence of applied electric field and thus contribute to the current, i.e., the photocurrent is decided by both the photo-excited carrier numbers and their transport probabilities reaching to collect area. According to Eq. (2), the gain is strongly dependent on the absorption coefficient α. For the device S1, efficient photo absorption occurs only in the GaN substrate. For the device S2, however, efficient photo absorption can occur in both the GZO contact layer and GaN substrate. At particular, strong photo absorption can take place in the solar blind spectral zone, as indicated in Fig. 4. The additional absorption in the GZO contact layer is the main reason why efficient photo responsivity is observed in the solar blind spectral zone for S2. The transport efficiency of the photo-excited carriers in the GaN substrates to the collection area of the two devices is reasonably similar. However, the probability in reaching the collection area of photo-excited carriers in the GZO thin film of S2 is increased as the GZO thin film itself also works as an electrode. This phenomenon is also favorable in explaining the observed enhancement of responsivity in the solar blind spectral zone for S2. In addition, it is probable that the type-II band alignment[22] and efficient carrier transfer at ZnO/GaN interface[23] also contributed to the interesting observed performance of the GZO/GaN photodetectors.

In conclusion, the two kinds of UV photodetectors were fabricated using different contact materials on GaN. Compared with the NiAu/GaN UV PDs, the GZO/GaN PDs show efficient responsivity in the solar blind spectral zone. The efficient photo absorption and transport efficiency of photo-excited carriers in the GZO contact layer are mainly responsible for the enhanced responsivity in the deep UV region.

This work was supported by the NSFC grant (No. 60977030) and the Joint Research Fund for Overseas Chinese, Hong Kong and Macau Scientists of NSFC (No. 61028012). One of the authors, RXW, wishes to thank Dr. T. F. Zhou, Dr. M. T. Niu, and Dr. X. H. Zeng for their technique assistance in the relevant measurements. Miss Z. Y. Xu was gratefully indebted by RXW for her editing and polishing the English of the manuscript.

[1]T. Saito, T. Hitora, H. Hitora, H. Kawai, I. Saito, and E. Yamaguchi, Phys. Status Solidi C **6**, S658 (2009).
[2]S. Zhang, D. G. Zhao, D. S. Jiang, W. B. Liu, L. H. Duan, Y. T. Wang, J. J. Zhu, Z. S. Liu, S. M. Zhang, and H. Yang, Semicond. Sci. Technol. **23**, 105015 (2008).
[3]S.-P. Chang, C.-Y. Lu, S.-J. Chang, Y.-Z. Chiou, T.-J. Hsueh, and C.-L. Hsu, IEEE J. Sel. Top. Quantum Electron. **17**, 990 (2011).
[4]D. B. Li, X. J. Sun, H. Song, Z. M. Li, H. Jiang, Y. R. Chen, G. Q. Miao, and B. Shen, Appl. Phys. Lett. **99**, 261102 (2011).
[5]Q. Chen, J. W. Yang, A. Osinsky, S. Gangopadhyay, B. Lim, M. Z. Anwar, M. Asif Khan, D. Kuksenkov, and H. Temkin, Appl. Phys. Lett. **70**, 2277 (1997).
[6]A. Motogaito, M. Yamaguchi, K. Hiramatsu, M. Kotoh, Y. Ohuchi, K. Tadatomo, Y. Hamamura, and K. Fukui, Jpn. J. Appl. Phys., Part 2 **40**, L368 (2001).
[7]E. Munoz, E. Monroy, J. L. Pau, F. Calle, F. Omnes, and P. Gibart, J. Phys.: Condens. Matter **13**, 7115 (2001).
[8]D. Walker, E. Monroy, P. Kung, J. Wu, M. Hamilton, F. J. Sanchez, J. Diaz, and M. Razeghi, Appl. Phys. Lett. **74**, 762 (1999).
[9]R. X. Wang, C. D. Beling, S. Fung, A. B. Djurišić, C. C. Ling, and S. Li, J. Appl. Phys. **97**, 033504 (2005).
[10]R. X. Wang, S. J. Xu, A. B. Djurišić, C. D. Beling, C. K. Cheung, C. H. Cheung, S. Fung, D. G. Zhao, H. Yang, and X. M. Tao, Appl. Phys. Lett. **89**, 033503 (2006).
[11]P. K. Nayak, J. Yang, J. Kim, S. Chung, J. Jeong, C. Lee, and Y. Hong, J. Phys. D **42**, 035102 (2009).
[12]J. K. Sheu, K. H. Chang, and M. L. Lee, Appl. Phys. Lett. **92**, 113512 (2008).

[13]D. C. Look, D. C. Reynolds, C. E. Litton, R. L. Jones, D. B. Eason, and G. Cantell, Appl. Phys. Lett. **81**, 1830 (2002).
[14]S. M. Sze, *Physics of Semiconductor Devices*, 2nd ed. (Wiley, New York, 1981).
[15]L. C. Yang, R. X. Wang, S. J. Xu, Z. Xing, Y. M. Fan, X. S. Shi, K. Fu, and B. S. Zhang, J. Appl. Phys. **113**, 084501 (2013).
[16]G. B. Palmer and K. R. Poeppelmeier, Solid State Sci. **4**, 317 (2002).
[17]M. Rebien, M. Hong, J. P. Mannaerts, and M. Fleischer, Appl. Phys. Lett. **81**, 250 (2002).
[18]J. J. Robbins, C. Fry, and C. A. Wolden, J. Cryst. Growth **263**, 283 (2004).
[19]J. A. Sans, A. Segura, J. F. Sánchez-Royo, V. Barber, M. A. Hernández-Fenollosa, and B. M. M. Orita, Superlattices Microstruct. **39**, 282 (2006).
[20]L. E. Brus, J. Chem. Phys. **80**, 4403 (1984).
[21]J. Singh, *Semiconductor Optoelectronic Physics and Technology* (McGraw-Hill, Inc., 1995).
[22]S.-K. Hong, T. Hanada, H. Makino, Y. Chen, H.-J. Ko, T. Yao, A. Tanaka, H. Sasaki, and S. Sato, Appl. Phys. Lett. **78**, 3349 (2001).
[23]J. Q. Ning, S. J. Xu, R. X. Wang, F. Zhang, H. Q. Le, and S. J. Chua, Jpn. J. Appl. Phys., Part 1 **48**, 021102 (2009).